Understanding and Targeting Coronaviruses: exploring advanced cell culture models and host-directed antiviral strategies

Thaler, M.

Chapter 3

SARS-CoV-2-infected human airway epithelial cell cultures uniquely lack interferon and immediate early gene responses caused by other coronaviruses

Melissa Thaler[1]*, Ying Wang[2]*, Clarisse Salgado-Benvindo[1], Nathan Ly[3], Anouk A Leijs[1], Dennis K Ninaber[2], Philip Hansbro[4], Fia Boedijono[4], Martijn J van Hemert[1], Pieter S Hiemstra[2], Anne M van der Does[2#], Alen Faiz[3#]

[1] Department of Medical Microbiology, Leiden University Medical Center, Leiden, the Netherlands

[2] PulmoScience Lab, Department of Pulmonology, Leiden University Medical Center, Leiden, the Netherlands

[3] University of Technology Sydney, Respiratory Bioinformatics and Molecular Biology (RBMB), School of Life Sciences, Sydney, Australia

[4] Centre for Inflammation, Centenary Institute and University of Technology Sydney, Faculty of Science, Sydney, Australia

* These authors contributed equally

# These authors share senior authorship

Running title: Unique transcriptional profile by SARS-CoV-2

Journal of Clinical & Translational Immunology, 13: e1503

Abstract

Severe acute respiratory syndrome coronavirus 2 (SARS-CoV-2) is a member of a class of highly pathogenic coronaviruses. The large family of coronaviruses; however; also includes members that cause only mild symptoms, like human coronavirus-229E (HCoV-229E) or OC43 (HCoV-OC43). Unravelling how molecular (and cellular) pathophysiology differs between highly and low pathogenic coronaviruses is important for the development of therapeutic strategies. Here, we analyzed the transcriptome of primary human bronchial epithelial cells (PBEC), differentiated at the air-liquid interface (ALI) after infection with SARS-CoV-2, SARS-CoV, Middle East Respiratory Syndrome (MERS)-CoV and HCoV-229E using bulk RNA sequencing. ALI-PBEC were efficiently infected by all viruses, and SARS-CoV, MERS-CoV and HCoV-229E infection resulted in a largely similar transcriptional response. The response to SARS-CoV-2 infection differed markedly as it uniquely lacked the increase in expression of immediate early genes, including *FOS*, *FOSB* and *NR4A1* that was observed with all other coronaviruses. This finding was further confirmed in publicly available experimental and clinical datasets. Interfering with NR4A1 signaling in Calu-3 lung epithelial cells resulted in a 100-fold reduction in extracellular RNA copies of SARS-CoV-2 and MERS-CoV, suggesting an involvement in virus replication. Furthermore, a lack in induction of interferon-related gene expression characterized the main difference between the highly pathogenic coronaviruses and low pathogenic viruses HCoV-229E and HCoV-OC43. Our results demonstrate a previously unknown suppression of a host response gene set by SARS-CoV-2 and confirms a difference in interferon-related gene expression between highly pathogenic and low pathogenic coronaviruses.

Keywords: primary airway epithelial cells; coronavirus; SARS-CoV-2; RNA sequencing; immediate early genes

Introduction

The outbreak of severe acute respiratory syndrome coronavirus 2 (SARS-CoV-2) that started late 2019 constituted an enormous threat to human health worldwide. Together with other highly pathogenic coronaviruses such as SARS-CoV and Middle East respiratory syndrome coronavirus (MERS-CoV), SARS-CoV-2 belongs to the genus *betacoronavirus* (β-CoV), of the *coronaviridae* family. These coronaviruses share many similarities but also exhibit evident differences. For human coronaviruses, the primary site of infection is the respiratory tract. However, there are marked differences in their host entry requirements, pathogenicity and

transmissibility (263). For example, the use of different host receptors for viral entry helps to explain differences in tissue tropism. SARS-CoV-2 furthermore demonstrates higher transmissibility, a wider range of clinical symptoms and lower mortality rates compared to SARS-CoV and MERS-CoV (263, 264). Not all human coronaviruses cause severe clinical symptoms. In fact, many of them only cause mild symptoms in healthy individuals. Human coronavirus 229E (HCoV-229E) (265), a member of the *alphacoronavirus* (α-CoV) genus, or human coronavirus OC43 (HCoV-OC43) (266), a member of the *betacoronavirus* genus, are two of the causative agents of the common cold. While HCoV-229E and HCoV-OC43 cause only mild symptoms in the upper respiratory tract of healthy people, SARS-CoV, SARS-CoV-2 and MERS-CoV may also infect the lower respiratory tract, resulting in a much wider range of respiratory illnesses and other non-pulmonary clinical manifestations that can be life threatening. It is important for the development of therapeutic strategies against infection with SARS-CoV-2, but also other (future) pathogenic coronaviruses, to understand the differences in their unique pathological characteristics.

RNA sequencing studies have shed light on many aspects of SARS-CoV-2 pathobiology. For example, bulk and single cell-RNA sequencing revealed the spatial distribution of cell entry factor expression and cell tropism (infection biology) within the respiratory epithelium (236, 267-269). Transcriptional analysis also showed differences between mild and severe COVID-19 cases and the diversity in immune responses (243, 270). Furthermore, infection of ciliated cells, the main cell type targeted by SARS-CoV-2, was demonstrated to lead to a significant downregulation of cilium assembly and motility pathways (267).

Despite our increasing knowledge on SARS-CoV-2 infection biology there are still important gaps in our understanding of what distinguishes SARS-CoV-2 from other coronaviruses in terms of pathogenesis and transmission. Comparing host responses during the initial phase of the infection of the respiratory epithelium between SARS-CoV-2 and other (highly pathogenic and low pathogenic) coronaviruses may provide important clues on how SARS-CoV-2 establishes its distinct effects.

Recent research has compared infectivity of various coronavirus strains in human nasal epithelial cultures (73), but this study did not provide insight into host transcriptional responses and was limited to the nasal region. Others have compared transcriptional responses to coronavirus infection by combining several independent datasets (271), or with only a limited number of different coronaviruses (272). Here we sought to determine the differences in the transcriptional response of well-differentiated primary bronchial epithelial cell cultures to infection with highly pathogenic SARS-CoV, SARS-CoV-2, MERS-CoV and low pathogenic HCoV-229E and in specific experiments also HCoV-OC43. Paired comparative analysis revealed differences between the host responses to these viruses and uncovered modulations of signaling pathways that were unique to SARS-CoV-2 infection.

Results

Successful infections of primary airway epithelial cells with SARS-CoV, SARS-CoV-2, MERS-CoV or HCoV-229E

To compare the transcriptional response of airway epithelial cells to various coronaviruses, we infected 6 week-differentiated ALI-PBEC (273) from 4 donors with an equal amount (~30,000 PFU) of either highly pathogenic SARS-CoV, SARS-CoV-2 or MERS-CoV, or low pathogenic HCoV-H229E. The relatively low amount of PFU was chosen to be representative for an initial infection (and subsequent spread over the tissue). Cultures were harvested at 6, 12, 24, 48 and 72 hpi followed by RNA isolation. RNA collected at 24, 48 and 72 hpi was subsequently used to perform bulk RNA-seq analysis (workflow is depicted in Figure **1a**). Viral replication was assessed by analysis of the RNA-seq datasets at 24, 48 and 72 hpi and additionally for each harvested time point (6, 12, 24, 48 and 72 hpi) by RT-qPCR analysis. The normalized viral genome counts (measured by RNA-Seq) of all coronaviruses showed a significant increase over the 72 h incubation period, with MERS-CoV having the highest observed increase (**Figure 1b**). These results were confirmed by quantification of intracellular viral RNA copies by RT-qPCR (**Figure 1c**). Furthermore, expression of genes encoding structural and non-structural proteins were increasing during infection time (**Figure 1d**) confirming active replication. A strong increase in subgenomic RNA encoding the most abundant viral protein N was observed for infections with all coronaviruses (**Figure 1d**).

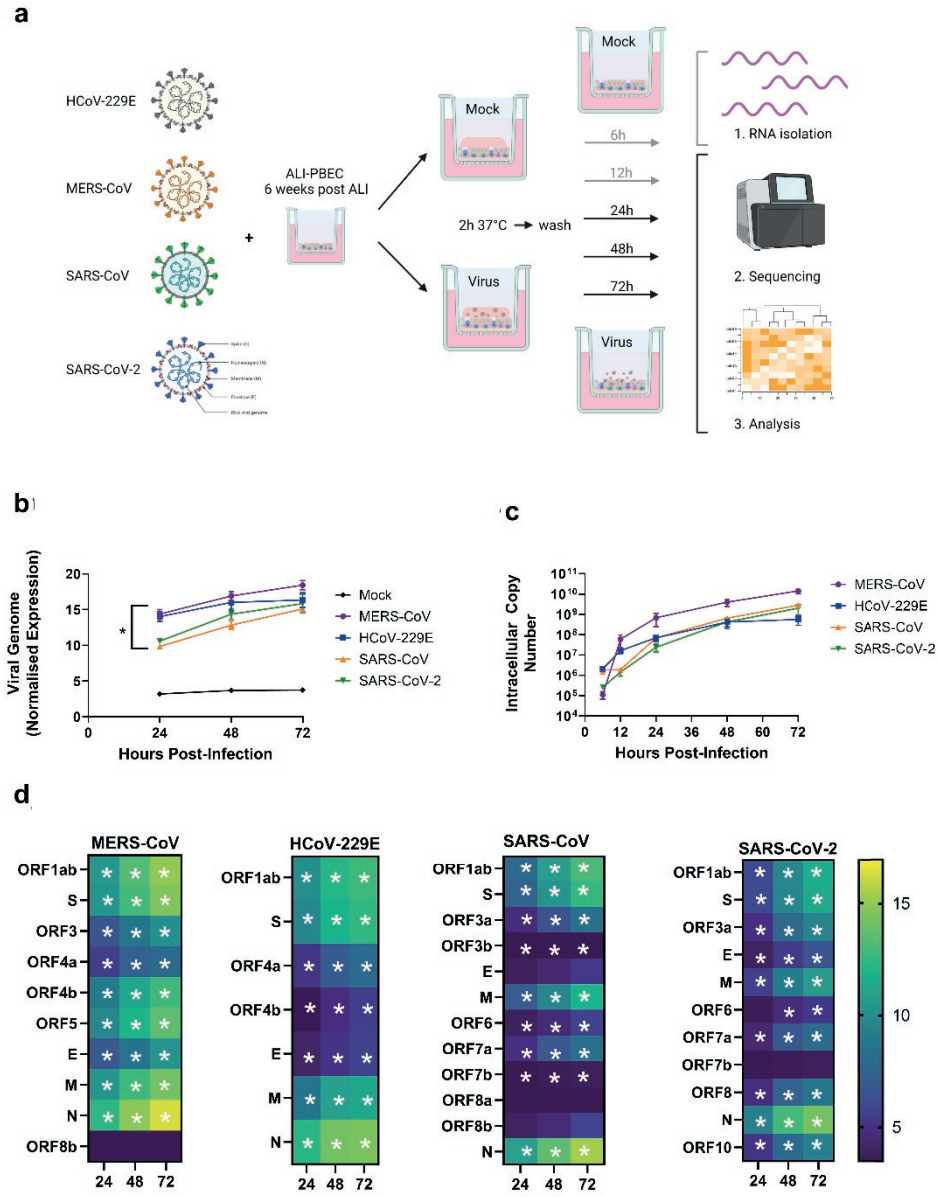

Figure 1: Experimental design and replication kinetics of several coronaviruses in ALI-PBEC. (a) Schematic diagram of experimental design and infection protocol. ALI-PBEC that were differentiated for 6 weeks were infected in parallel with four different coronaviruses. At several time-points after infection RNA was harvested from these cultures and RNA from the 24, 48 and 72h time points was analyzed by bulk RNA-seq. (b) Replication of coronaviruses in ALI-PBEC over the 72h period was assessed by mapping the viral sequences in the bulk RNA-seq dataset. Significant differences between virus and mock for all time-points was assessed using a two-way ANOVA followed by an unprotected Fisher's least significance difference test and (c) intracellular viral RNA copies

at each time-point were measured by RT-qPCR. (d) Viral reads were mapped against the respective genome sequence and changes in the abundance of sequences mapping to the various viral open reading frames during infection are summarized. Statistics were conducted using a paired edgeR differential expression analysis comparing all viruses to mock. Data are shown as mean ± SEM of cultures derived from $n = 4$ different donors and differences were considered significant at $P < 0.05$. Figure 1a was created with BioRender.com.

Gene expression of entry-related factors is changed during coronavirus infection of airway epithelial cells

A principal component analysis (PCA) of the complete RNA-seq dataset demonstrated that samples clustered based on donor ID (**Figure 2a**). This finding is not unexpected and could be explained by differences in cell composition of the cultured airway epithelium between donors. Cellular deconvolution of these samples showed that each donor had a distinct profile of ciliated, mucosecretory and basal cells (**Figure 2b**), which was not altered by the different coronavirus infections (Supplementary **Figure 1**). Next, we focused on the expression of known coronavirus entry-related factors and determined whether changes occurred during infection (**Figure 2c**). Overall, we mostly observed a decrease in expression of these genes during infection, except for SARS-CoV-2. Angiotensin converting enzyme 2 (*ACE2*) and transmembrane serine protease 2 (*TMPRSS2*), the genes encoding for the main viral entry receptor and protease that cleaves the SARS-CoV-2 S-protein for subsequent cell entry, respectively, were not significantly altered in most of our samples. Significant changes were only found for *TMPRSS2* at later time-points in SARS-CoV (48 hpi) and MERS-CoV (72 hpi) infection, compared to mock-infected controls. Cathepsin L (*CTSL)* expression declined significantly over time in MERS-CoV and HCoV-229E-infected cultures, while *Furin* expression increased. Neuropilin-1 (*NRP1*), which was described as a co-receptor for SARS-CoV-2 cell entry (274) showed an increase in expression at 24 h and 48 h after SARS-CoV-2 infection, but then declined at 72 hpi (**Figure 2c**). Together these data indicate that infection results in shifts in expression of various factors involved in coronavirus entry, which may mediate further spread upon initial infection in the epithelial cultures.

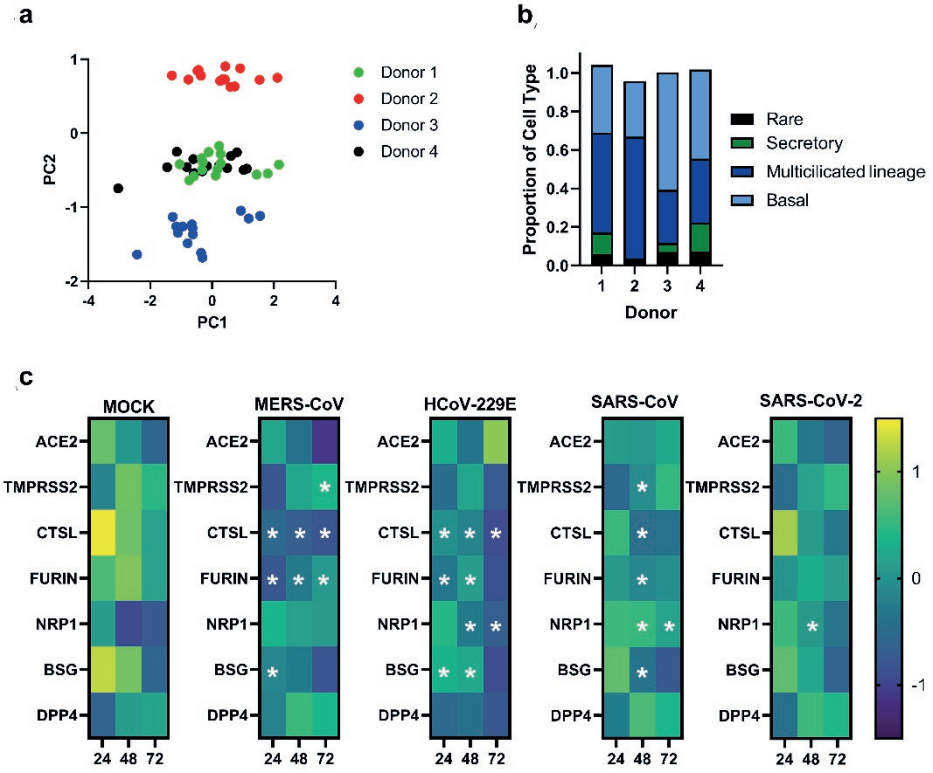

Figure 2: Donor-dependent clustering of samples, cellular composition and expression of viral entry-related genes in well-differentiated ALI-PBEC. PBEC that were differentiated for 6 weeks at ALI were infected in parallel with four different coronaviruses. (a) PCA of transcriptional profiles of all cell culture samples over time of infection. (b) Relative proportion of different cell types for each donor determined by cellular deconvolution of the transcriptomic dataset. (c) Changes in expression of common viral entry-related genes over time of infection (n = 4). Statistics were conducted using a paired edgeR differential expression analysis comparing all viruses to mock where a *P-value < 0.05 was considered significant.

Increased immediate early gene expression by airway epithelial cells infected with SARS-CoV, MERS-CoV and HCoV-229E

Before addressing the SARS-CoV-2 transcriptional profiles, we first compared the expression profiles of ALI-PBEC in response to SARS-CoV, MERS-CoV and HCoV-229E at 24, 48 and 72 hpi. ALI-PBEC infected with SARS-CoV showed significant different expression of 80 genes at 24 hpi, compared to the control, of which 69 were increased in expression and 11 decreased in expression. In MERS-CoV-infected cells, we identified 934 differentially

expressed genes, of which 580 were increased and 354 decreased in expression at 24 hpi. Cells infected with HCoV-229E displayed an increased expression of 433 genes and reduced expression of 162 genes at 24 hpi (FDR<0.05, FC>1.5). The significantly changed genes at 24 hpi are depicted in volcano plots in **Figure 3a-c** and **Table S3** (results of the other time-points (48 h and 72 h) are included in Supplementary **Figure 2**) and the total expression profiles over time in **Figure 3d**. A specific set of genes (see methods section) was significantly increased at all time-points after start of infection with SARS-CoV, MERS-CoV and HCoV-229E. Many of these belong to a group of well-known genes, called immediate early genes (IEGs), which play an important role in the cell's rapid response to its external environment (275). The remarkable overlap in these genes between ALI-PBEC infected with SARS-CoV, MERS-CoV or HCoV-229E (**Figure 3e** and Supplementary **Figure 2**) was dominated by *FOS*, *NR4A1* and *FOSB* gene expression and their increased expression was extracted from the RNA-seq dataset (**Figure 3e**) and supported by RT-qPCR analysis of these genes (**Figure 3f**). To confirm our findings, we investigated *FOS*, *NR4A1* and *FOSB* gene expression also in two publicly available datasets of primary airway epithelial cells and Calu-3 cells infected with MERS-CoV and SARS-CoV, respectively (**Figure 3g-h**). These datasets supported our results showing upregulation of *FOS*, *NR4A1* and *FOSB* gene expression following MERS-CoV and SARS-CoV infection (**Figure 3g-h**). Together these results indicate an activation of the expression of specific IEGS by these coronaviruses and their sustained high level of expression for at least 72 hpi.

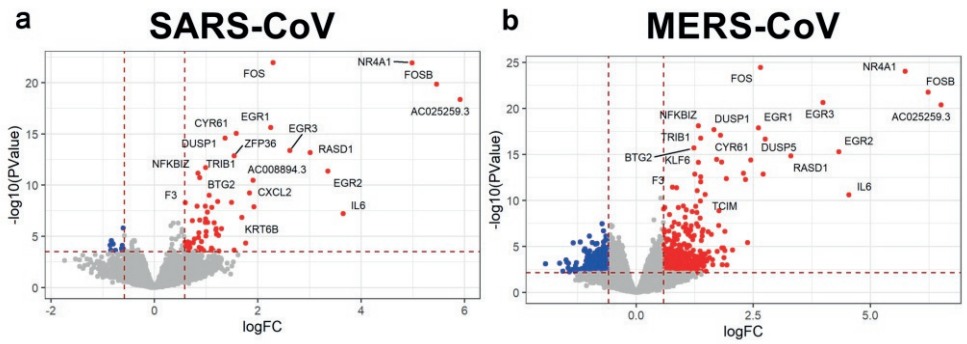

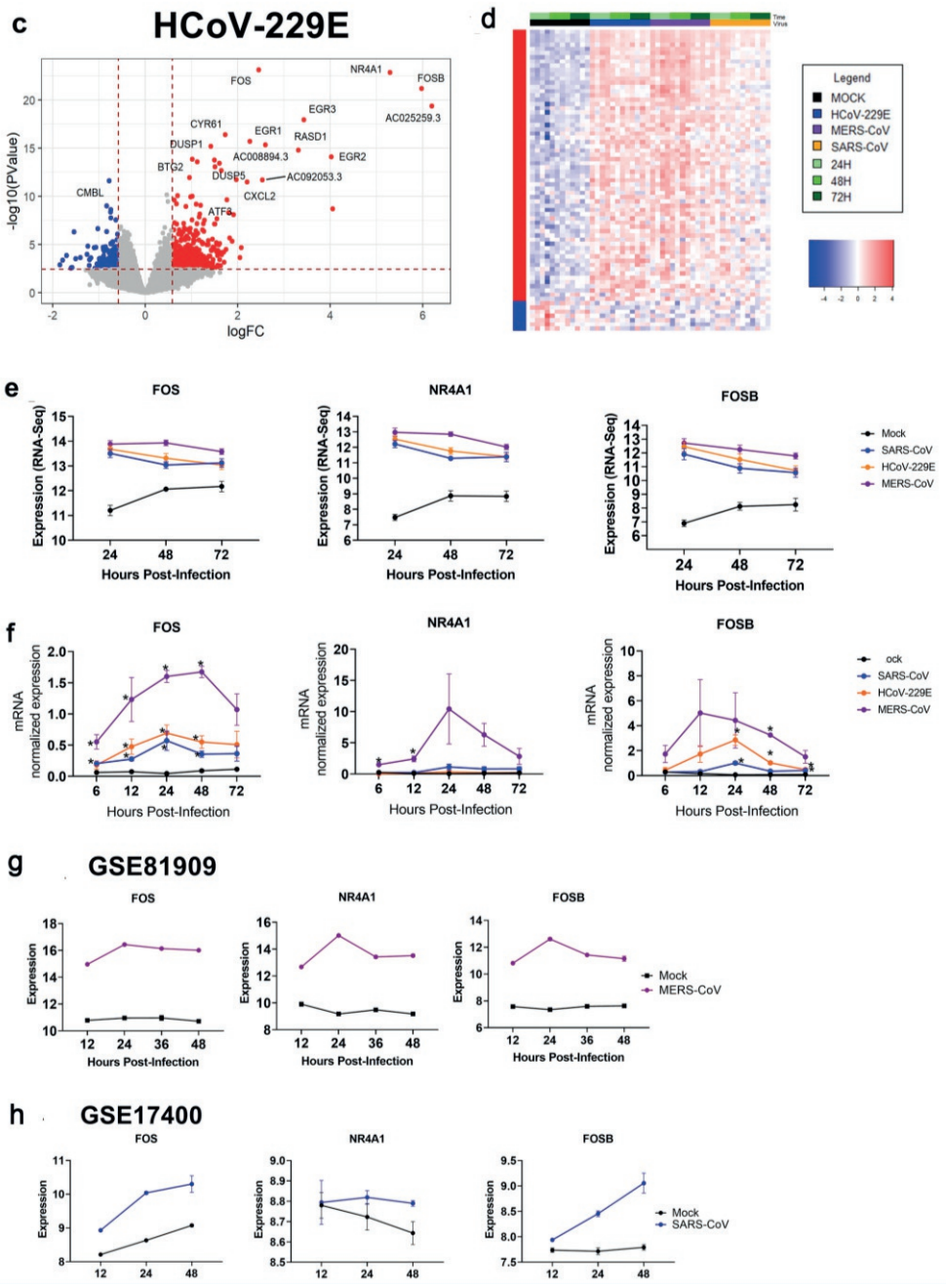

Figure 3: Gene expression profiles of well-differentiated primary bronchial epithelial cell cultures infected with three different coronaviruses. (a) Volcano plots depicting gene expression profiles of bronchial epithelial cell cultures infected with (a) SARS-CoV (b) MERS-CoV or (c) HCoV-229E at 24 hpi in comparison to the uninfected

controls. Red dots indicate significantly upregulated genes and blue dots indicate significantly downregulated genes. (d) Heatmap of significantly changed genes during infection with SARS-CoV, MERS-CoV or HCoV-229E and mock as uninfected control (log2fold change> |1.5| and FDR<0.05). (e) Changes in gene expression of FOS, NR4A1 and FOSB during infection with three different coronaviruses using data from the RNA-seq analysis. (f) The same genes as in Figure 3E were analyzed for all harvested time-points using traditional qPCR. Data are expressed as normalized values for *ATP5B* and *OAZ1*. (g) A publicly available microarray dataset (GSE81909) was used to analyze the impact of MERS-CoV infection on these three IEGs in primary airway epithelial cells. (h) A publicly available dataset (GSE17400) was assessed to analyze the effect of SARS-CoV infection on these IEGs in Calu-3 cells during 48 h with an MOI of 0.1. Data from a-f were from $n = 4$ different donors. Significant differences between virus infection and mock for all time-points was assessed using a two-way ANOVA followed by an unprotected Fisher's least significance difference test, $*P < 0.05$ was considered significant, data from e-h are depicted as mean ± SEM.

Airway epithelial cells infected with SARS-CoV-2 display a distinct transcriptional response that lacks induction of immediate early genes

Next, we addressed the specific transcriptional responses of ALI-PBEC cultures following SARS-CoV-2 infection. Strikingly, gene expression analysis identified that despite a viral load that was comparable to the other viruses, no genes were significantly changed at 24 and 48 hpi (data not shown). At 72 hpi, there were no significantly increased genes while a decrease in 3 genes was observed (*FOS*, *NR4A1* and *FOSB)* (**Figure 4a**, **Table S4**). These results show that SARS-CoV-2-infected ALI-PBEC lack the increased IEG expression that was observed for the other coronaviruses, while even a decrease in the gene expression of *FOS*, *NR4A1* and *FOSB* in SARS-CoV-2-infected ALI-PBEC was observed (**Figure 4b**). Using RT-qPCR, we confirmed that over the time course of 6-72 hpi there was no increase in expression of these genes (**Figure 4c**). Only *FOS* mRNA expression was increased at 48 hpi compared to mock infection. However, compared to the other three coronaviruses, the upregulation of *FOS* expression by SARS-CoV-2 was minimal, and not supported by the results of the RNA-seq data. Furthermore, we conducted an analysis of signature genes increased by SARS-CoV, MERS-CoV and HCoV-229E at all time points (included genes are listed in the methods section). It was evident from this analysis that SARS-CoV-2 did not increase these genes to the same extent as the other coronaviruses did and even appeared to actively suppress them compared to the control group (**Figure 4d**). This signature gene set was furthermore validated to be changed in MERS-CoV and SARS-CoV infections reported in publicly available datasets (**Figure 4e-f**).

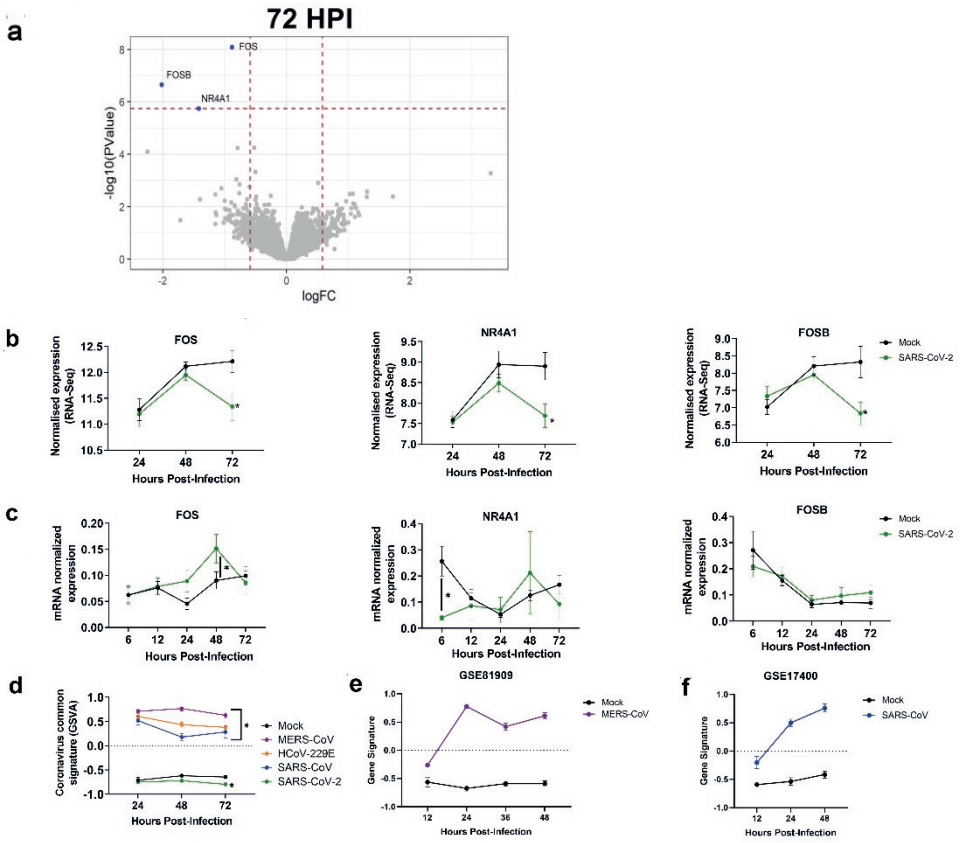

Figure 4: Gene expression profiles of well-differentiated primary bronchial epithelial cells during SARS-CoV-2 infection. (a) Volcano plot depicting gene expression profiles of bronchial epithelial cell cultures infected with SARS-CoV-2 at 72 hpi (*n* = 4). (b) The expression of FOS, *NR4A1* and *FOSB* over a 72h infection period with SARS-CoV-2 using data from the RNA-seq analysis (*n* = 4). (c) The same genes as in figure b were analyzed for all time-points using traditional qPCR. (d) Comparison of a MERS-CoV, SARS-CoV, HCoV-229E signature gene set between all coronavirus infected cultures at 24, 48 and 72 hpi (*n* = 4). (e) A publicly available microarray dataset (GSE81909) was assessed to analyze the impact of MERS-CoV infection on the MERS-CoV, SARS-CoV, HCoV-229E signature gene set. (f) A publicly available dataset (GSE17400) was assessed to analyze the effect of SARS-CoV infection on the MERS-CoV, SARS-CoV, HCoV-229E signature gene set. Significant differences between virus infection and mock for all time-points was assessed using a two-way ANOVA followed by an unprotected Fisher's least significance difference test, $*P < 0.05$ was considered significant, data from b-f are depicted as mean ± SEM.

Validation of the effects of SARS-CoV-2 on immediate early gene expression by lung epithelial cells

To better understand and confirm our findings, we further investigated publicly available datasets. First, we analyzed the total IEG gene set in three publicly available RNA-seq datasets, derived from bronchial or alveolar epithelial cells infected with SARS-CoV-2 for various time-points, of which none showed a significant change in gene expression (**Figure S4**) compared to the uninfected control. Next, we analyzed these datasets to specifically assess the expression of the most prominently changed genes in our dataset, including *FOS*, *FOSB* and *NR4A1*. In the first dataset: GSE153970, collected from primary human airway epithelial cells cultured at ALI, (infected with SARS-CoV-2 at an MOI of 0.25 and analyzed at 48 hpi) a significant decrease in *FOS* gene expression was found in SARS-CoV-2-infected cultures, accompanied by a lack in upregulation of *FOSB* and *NR4A1* (**Figure 5a**), mirroring our results. Similar results for *FOS* (**Figure 5b**) expression were found at 48 hpi in primary lung alveolar type-2 epithelial cells in a 3D organoid culture infected with SARS-CoV-2 (GSE155518; **Figure 5b**). Finally, we validated our findings using a dataset that originated from a study on SARS-CoV-2 infection of ALI-PBEC, that included samples harvested at 6-96 hpi (GSE175779; **Figure 5c**). This dataset displayed no significant increase in *FOS*, *NR4A1* and *FOSB* gene expression (only a decrease at 48 hpi for *FOSB*) over the 96 h course of infection (**Figure 5c**), like all other SARS-CoV-2 datasets.

To understand if the observed differences in the changes of these specific genes between SARS-CoV-2 and the other coronavirus-infected cultures were a consequence of a difference in viral load or kinetics, we also analyzed cultures that were infected with a higher dose, 10^6 PFU, of SARS-CoV-2 (estimated MOI of 1). We followed gene expression levels in this culture for a longer period, up to 7 days post infection. We assessed viral replication and changes over time using plaque assay and RT-qPCR. Analysis of infectious virus produced over seven days showed a peak in the accumulation of infectious progeny at 4-5 days post infection with more than 10^6 PFU/ml, and a corresponding strong increase in intracellular viral RNA up to 3 days p.i. (**Figure 5d**). We furthermore detected a significant increase in *NR4A1* expression from 3-5 days post infection (**Figure 5e**) and a slight increase in *FOSB* expression at day 4 after SARS-CoV-2 infection while no effects on *FOS* expression was observed (**Figure 5e**), suggesting a delayed response to SARS-CoV-2. Nevertheless, despite these changes, the increased expression of these genes observed at later time points with a higher MOI was still substantially lower than upon infection with SARS-CoV, MERS-CoV or HCoV-229E in the original experiments where a lower MOI was used. To obtain further insight, we also assessed IEG expression in publicly available datasets of infected cultures and individuals analyzed with single-cell RNA sequencing. In well-differentiated human PBEC cultures

infected with SARS-CoV-2 and analyzed at 7 days post-infection, single-cell RNA sequencing results showed that resting basal and multiciliated cells had a significantly lower enrichment score for the IEG gene set in infected cells compared to non-infected cells (**Figure 5f**). Finally, we assessed IEG expression in a clinical dataset that was generated by nucleo-seq analysis of cells derived from deceased uninfected or SARS-CoV-2-infected individuals. Confirming our findings, no increase in IEG gene expression was observed. In alveolar type-2 epithelial cells, differentiating and mature lymphatic endothelial cells, and monocytes showed a significantly lower enrichment score in infected compared to non-infected individuals, while secretory epithelial cells showed a strong trend (**Figure 5g**). Together these results demonstrate that, unlike all other coronaviruses tested, SARS-CoV-2 does not induce and might even actively suppress IEG expression in epithelial cells and potentially other cell-types.

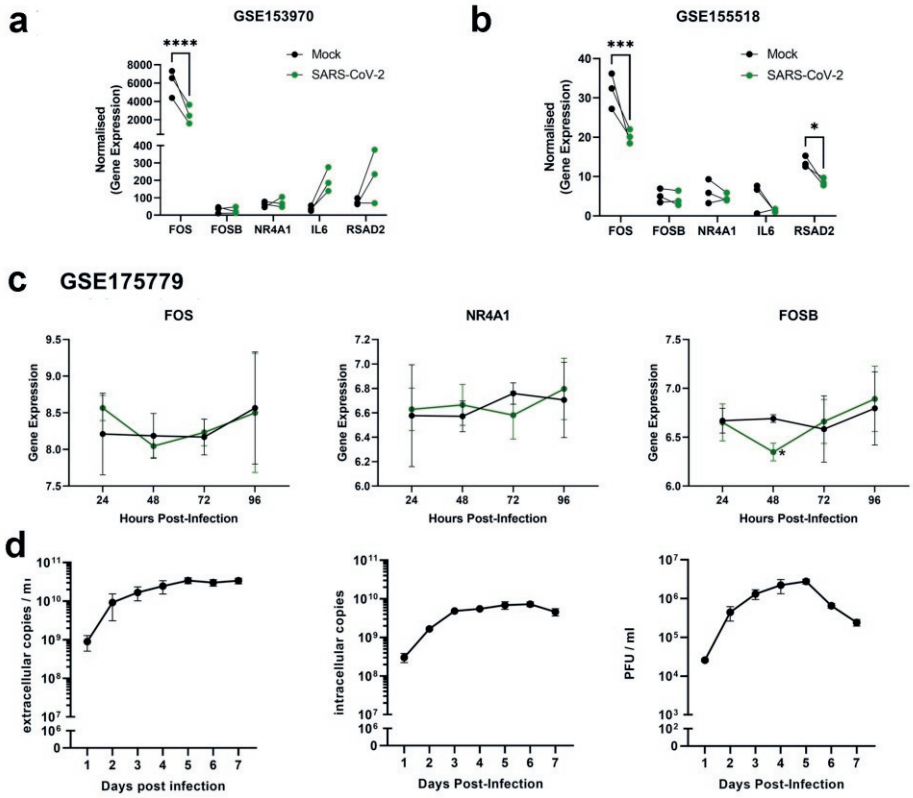

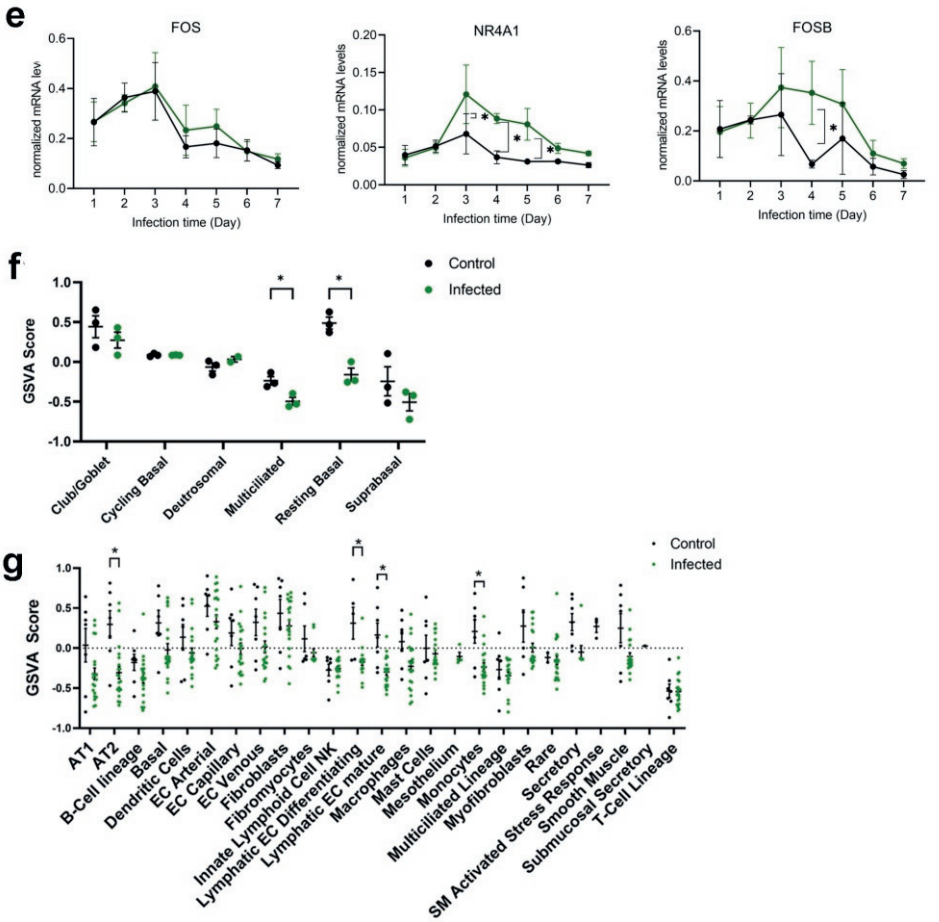

Figure 5: Analysis of IEG expression upon SARS-CoV-2 infection of epithelial cells in public datasets and in long-term infection. (a) A publicly available dataset (GSE153970) with RNA-seq analysis on primary epithelial cell cultures mock-infected or infected with SARS-CoV-2 at a MOI=0.25 at 48 hpi was analyzed for *FOS, NR4A1* and *FOSB* expression. (b) A publicly available dataset (GSE155518) derived from primary human lung alveolar epithelial organoid cultures infected with SARS-CoV-2 was analyzed for *FOS, NR4A1* and *FOSB* expression. (c) A publicly available dataset (GSE175779) from primary human bronchial epithelial cells infected with SARS-CoV-2 over a 96 h infection period was analyzed for *FOS, NR4A1* and *FOSB* expression. (d) RT-qPCR measurement of extracellular (left graph) and intracellular viral RNA (middle graph), and plaque assay measurement of infectious virus particles (right graph) in the apical wash of SARS-CoV-2 infected ALI-PBEC over 7 days; $n = 3$ independent donors. (e) The expression of IEGs was measured by qPCR in ALI-PBEC infected with SARS-CoV-2 for 7 days. Data are shown as mean ± SEM; $n = 3$ independent donors. Significant differences between virus infection and mock for all time-points was assessed using a two-way ANOVA followed by an unprotected Fisher's least significance difference test, $*P < 0.05$ was considered significant, data are depicted as mean ± SEM. (f) GSVA analysis of the IEG gene set on a publicly available single-cell RNA-Seq dataset (269) from well-differentiated human bronchial epithelial cell cultures infected with SARS-CoV-2 and analyzed 7 days post infection. Significant differences between infected and uninfected cultures was tested using a two-way ANOVA with Bonferroni correction$*P < 0.05$ was considered

significant (g) GSVA analysis of the IEG gene set on a publicly available Nucleo-Seq dataset (276) from cells derived from tissue from deceased COVID-19 patients and deceased uninfected individuals. Significant differences between infected and uninfected individuals per cell-type was tested using an unpaired T-test with Bonferroni correction. *P <0.05 was considered significant.

NR4A1 antagonist suppresses coronavirus replication

Since *FOS*, *FOSB* and *NR4A1* gene expression was consistently lacking in epithelial transcriptional responses to SARS-CoV-2, we next investigated their contribution to viral infection by modulation of their activity, or modulation of related signaling pathways, using small molecules. FOS and FOSB are associated with the JNK/AP1 pathway, therefore based on literature, we selected the compounds Sp600125 (JNK inhibitor) and T-5224 (AP-1 transcription factor inhibitor) to modulate this pathway. We furthermore selected DIM-C-pPhOH (NR4A1 antagonist) and Cytosporone B (NR4A1 agonist) for modulation of the NR4A1 pathway. We compared the effects of these compounds in SARS-CoV-2 and MERS-CoV infected Calu-3 cells, since the increase in expression of the associated IEG genes was most pronounced after MERS-CoV infection while it was absent after SARS-CoV-2 infection. Sp600125, T-5224 and Cytosporone B had no effect on viral replication in viral load reduction assays with Calu-3 lung epithelial cells (**Figure 6**). Interestingly, DIM-C-pPhOH, which inhibits the activity of nuclear receptor 4A1 (NR4A1), resulted in a two-log reduction of extracellular viral RNA copies for SARS-CoV-2 as well as MERS-CoV infected cells (**Figure 6**). When we treated uninfected cells in parallel, we observed no cytotoxicity with 10 µM of DIM-C-pPhOH (Supplementary **figure 3**). The inhibitory effect of the modulation of NR4A1 activity on virus replication suggests its possible involvement in infection biology.

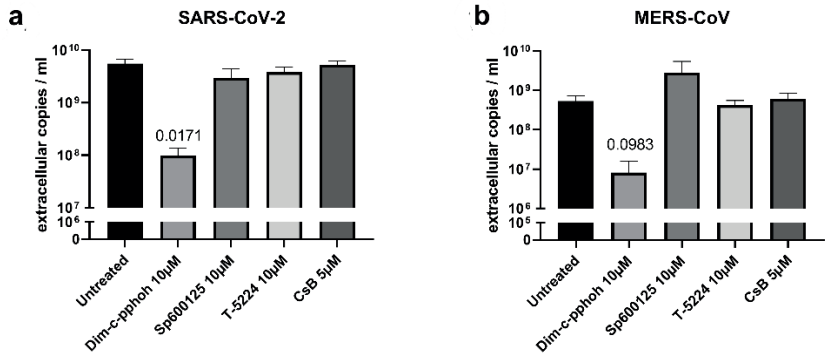

Figure 6: Effect of compounds that modulate pathways related to IEGs on SARS-CoV-2 and MERS-CoV infection. (a) Effect of compounds that modulate pathways related to JNK/AP-1 pathway and NR4A1 on SARS-CoV-2 and (b)

MERS-CoV infection in Calu-3 cells. DIM-C-pPhOH (NR4A1 antagonist), Sp600125 (JNK inhibitor), T-5224 (AP-1 transcription factor inhibitor) and Cytosporone B (CsB; NR4A1 agonist). Calu-3 cells were preincubated for 1 h with these compounds and subsequently infected with SARS-CoV-2 or MERS-CoV (MOI of 1) in 150 µl infection medium for 1 h. After 24 h of incubation with compounds supernatants were harvested. Extracellular copies were measured by RT-qPCR. Data are shown as mean ± SEM. *n* = 4 independent experiments for SARS-CoV-2 and *n* = 3 independent experiments for MERS-CoV, except for Sp600125 *n* = 2 independent experiments were performed for both viruses. Statistical significance was tested between a compound and the untreated control using a two-tailed paired *t*-test. The *P*--value is indicated in the graph and is considered significant <0.05.

Difference in transcriptional responses between primary bronchial epithelial cultures infected with highly pathogenic and low pathogenic coronaviruses

To improve our understanding on why some coronaviruses are highly pathogenic while others are low pathogenic, we next compared transcriptional responses of epithelial cultures infected with highly pathogenic coronavirus strains (i.e., SARS-CoV; SARS-CoV-2 and MERS-CoV) with those infected with low pathogenic HCoV-229E and HCoV-OC43. We originally only included HCoV-229E in the comparison, since HCoV-OC43 does not infect bronchial epithelial cells at 37°C. However, to increase the power of our observations with low pathogenic coronaviruses, we next performed independent additional experiments at 33°C using the same donors but infected them with HCoV-OC43 (see Methods section). At 24 hpi we detected 5 significantly changed genes with 4 genes decreased in expression and one gene increased. The four decreased genes included (AL022323.4 (KIAA1671)), a protein with -to our knowledge- no known function in the context of highly pathogenic coronaviruses and *CARNS1*, *EPX* and *MIR210HG*. The one gene that was increased in expression was *CLDN8*. At 48 and 72 hpi, we identified 397 and 744 genes significantly different, respectively (**Figure 7a-d**, **Table S5**). We observed that both HCoV-229E and HCoV-OC43 induced a stronger interferon response than coronaviruses that are highly pathogenic (**Figure 7e**). Notably, the experiments in which infection with HCoV-OC43 was performed at 33°C also included SARS-CoV-2 as a control, to account for the possibility that the temperature affects the host immune response. When we investigated the expression of each interferon individually, IFN-β1 was undetectable and no significant differences were observed in IFN-α1; however; IFN-λ1 was found to be expressed higher in HCoV-229E and HCoV-OC43 at 72 h than coronaviruses that are highly pathogenic (**Figure 7f-g**). This evasion of IFN responses has been described for highly pathogenic coronaviruses (109, 277) and may explain why the host is more readily able to fight off an infection with HCoV-229E or HCoV-OC43. To support that this difference in gene expression profiles related to interferon has functional consequences for infection, we infected ALI-PBEC with SARS-CoV-2 and treated these cultures with IFN-λ1 right at the start of infection. We found that this indeed

lowered the level of SARS-CoV-2 in the cultures as the IFN-λ1 treatment led to >1 log reduction in viral load in all four tested donors compared to the untreated infected cultures (**Figure 7h**). Together these data demonstrate that the suppression of IFNs by SARS-CoV-2 favors its replication, which is also likely for the other high-pathogenic viruses.

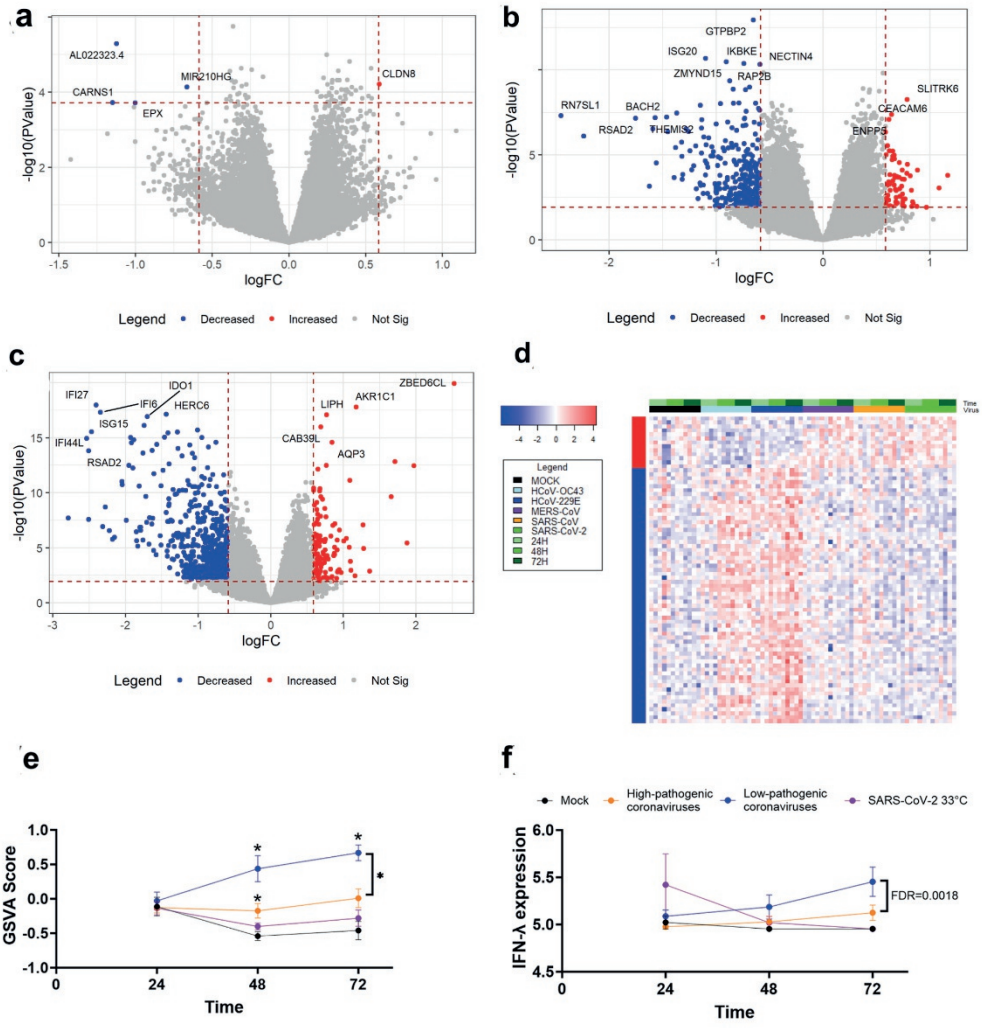

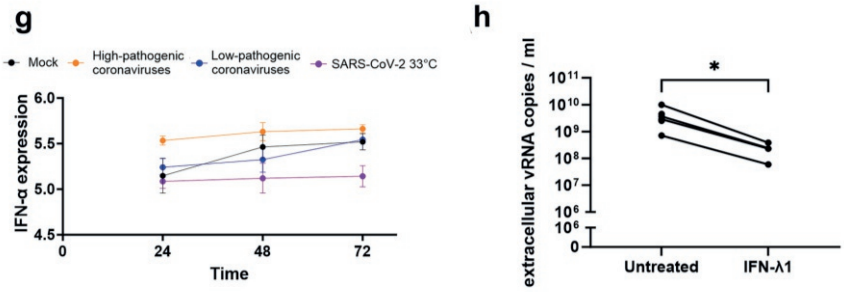

Figure 7: Analysis of interferon (-response) genes upon coronavirus infection and effects of IFN-λ1 supplementation on viral load. (a) Volcano plots depicting shared gene expression profiles of bronchial epithelial cell cultures infected with SARS-CoV, SARS-CoV-2 or MERS-CoV for (a) 24, (b) 48 hpi or (c) 72 hpi in comparison to HCoV-229E and HCoV-OC43; *n* = 4. Red dots indicate significantly upregulated genes and blue dots indicate significantly downregulated genes. (d) Heatmap of the overlap of significantly changed genes during 24, 48 and 72 hpi infection with SARS-CoV-2, SARS-CoV, MERS-CoV or HCoV-229E or HCoV-OC43 and mock as uninfected control. (e) Gene set variation analysis (GSVA) was performed on interferon response genes after 24, 48 and 72 hpi (*n* = 4) in highly pathogenic (orange) and low pathogenic (blue) coronavirus-infected cultures. As HCoV-OC43 infection was conducted at 33°C, SARS-CoV-2 infection at 33°C was included as control (pink). (f) IFN-λ1 and (g) IFN-α1 gene expression after 24, 48 and 72 hpi (*n* = 4) in highly pathogenic (orange) and low pathogenic (blue) coronavirus-infected cultures. The error bar indicates the standard deviation. Significant difference in increased gene expression over time of infection ($P < 0.05$) are shown by the * symbol. Two-way ANOVA followed by an unprotected Fisher's least significance difference test was conducted to test for significance. (h) ALI-PBEC cultures were pre-treated with 5 ng mL^{-1} interferon-lambda (IFN-λ1) for 60 min and subsequently infected with SARS-CoV-2 for 3 days with IFN-λ1 present in the basal medium. Extracellular viral RNA copies are depicted in log scale. Data in Fig. 7h are tested with a paired *t*-test and are depicted as mean ± SEM. *n* = 4 independent donors.

Discussion

Here we report marked differences in the transcriptional response of primary human bronchial epithelial cells to infection with SARS-CoV-2 when compared to infection with other highly pathogenic and low pathogenic coronaviruses. Infection with SARS-CoV, MERS-CoV and low pathogenic HCoV-229E evoked a partially overlapping transcriptional response, characterized by a significant and sustained increase in expression of IEGs such as *FOS*, *NR4A1* and *FOSB.* In contrast, the response to SARS-CoV-2 infection was characterized by the absence of such an increase and the only DEGs in the SARS-CoV-2 dataset that were significantly downregulated at 72 hpi were *FOS*, *NR4A1* and *FOSB*. Infection with SARS-CoV-2 at a higher MOI and prolonged incubation, i.e. for 7 days, did also not lead to an increase in the expression of the genes that were upregulated during SARS-CoV, MERS-CoV or HCoV-229E infection. We furthermore confirmed the increased

expression of these IEGs by MERS-CoV and SARS-CoV and the lack thereof by SARS-CoV-2 infection in publicly available data sets, including a clinical dataset. Treatment of infected cells with an NR4A1 antagonist decreased viral load, suggesting that the differential IEG gene expression may contribute to the kinetics of infection and potentially the pathogenicity of coronaviruses. Furthermore, we observed that activation of genes involved in interferon signaling was readily induced upon infection with the low pathogenic HCoV-229E and HCoV-OC43, whereas no such induction was observed with the three highly pathogenic coronaviruses, including SARS-CoV-2.

Where others have focused on the pathways that are activated by SARS-CoV-2 infection (278), the comparison between SARS-CoV-2 and other coronaviruses performed here highlight that SARS-CoV-2 may suppress or not induce expression in pathways that are activated by other coronaviruses. Many of the genes that were upregulated in cells infected with SARS-CoV, MERS-CoV and HCoV-229E, but not SARS-CoV-2, were IEGs. It still remains a question whether SARS-CoV-2 actively suppresses expression of these genes or lacks the ability to induce their expression. IEGs are a group of genes with various functional activities that are coordinately and rapidly upregulated in response to a diverse set of stress or proliferation-inducing stimuli. Their expression does not require *de novo* synthesis of proteins encoded by other genes, explaining their rapid induction. Besides being an IEG itself, recently it was established that *NR4A1* also regulates expression of IEGs (279), in particular, NR4A1 suppresses expression of IEGs including *FOS* and *FOSB*. This demonstrates the complexity of the signaling regarding these IEGs. In our study, we treated Calu-3 cells with the NR4A1 inhibitor DIM-C-pPhOH, thereby mimicking the putative SARS-CoV-2-mediated suppression of NR4A1 activation and found reduced replication of both SARS-CoV-2 and MERS-CoV. Nevertheless, it should be noted that despite the differences in IEG expression levels, the extent of infection was similar in all coronavirus-infected cultures. Therefore, it is more likely that the suppression of IEGs is affecting the inflammatory/immune response following epithelial infection rather than the viral levels. Furthermore, several of these IEGs such as *FOS* and *FOSB* are related to the JNK/AP-1 pathway, which has an essential role in cell death of infected cells via apoptosis and necrosis, and is important for the cellular response to pro-inflammatory stimuli, and thus could limit progression of infection (280). It is additionally involved in innate and adaptive immunity through for example, its relation to NF-κB (281). The lack of the pro-apoptotic function and regulatory role of the inflammation response of JNK/AP-1 related pathways could lead to prolongation of SARS-CoV-2 infection and/or delayed symptom development, especially early in infection. It may also contribute to the dysregulation of cytokine and chemokine responses. How SARS-CoV-2 exactly inhibits expression of IEGs will be of interest for further studies as the complexity of regulation of these IEGs requires in-depth analysis.

Activation of the JNK/AP-1 signaling pathway also occurs in response to other respiratory viruses like influenza or RSV (282, 283), and small-molecule inhibitors of this pathway were even shown to act as antivirals against influenza infection (284). Also treatment with the NR4A1 agonist cytosporone B controlled Influenza A replication via regulation of anti-viral responses in mice (285). Studying the role of IEGs in virus replication and infection biology is therefore interesting beyond coronaviruses.

Further research is needed to evaluate donor differences in the observed changes in gene expression in response to the variable coronaviruses. Our dataset only included a limited number of donors, with variable cellular composition. Unfortunately, we had to eliminate one donor from our dataset as it did not display transcriptional responses to infection with any of the viruses. We have repeated the SARS-CoV-2 infection with cells from the same donor and then comparable responses were found between donors using targeted PCR reactions, suggesting that a technical issue in the RNA sequencing explained these findings with this donor. To overcome the limitation of having included only 4 donors, we validated the outcomes in several publicly available datasets, we assessed expression of both the whole IEG gene set and several individual DEGs, in these datasets, which supported our findings. Importantly, the single cell RNA sequencing dataset confirmed that the absence of IEG expression that we detected in our SARS-CoV-2-infected cultures was also present in samples from infected humans. We furthermore confirmed the lack in IEGs expression by SARS-CoV-2 in the additional donors (not included in the RNA sequencing data set) that were tested in the prolonged infection experiment, in which also more virus was used to infect the cells. We can, however, not exclude that -in addition to the observations reported in this study- additional differences may have been missed as a result of the relatively low number of replicates. We can also formally not exclude that the presence of a tumor in the lung tissue has affected the surrounding tumor-free tissue from which the bronchial epithelial cells were isolated; however; obtaining lung tissue from healthy donors is a challenge for obvious reasons. We have validated our findings in datasets of others and could confirm our findings, and therefore we think that the use of this type of tissue has not affected our conclusions. The fact that we used a SARS-CoV-2 isolate from the first wave of the pandemic, and not the less pathogenic Omicron variant of SARS-CoV-2, can be viewed as a limitation. However, we specifically aimed to understand how highly pathogenic SARS-CoV-2 variants that cause severe disease redirect epithelial responses, also in view of preparedness for future pandemics.

We also aimed for functional translation of the effects found on interferon genes. However, to translate what we observed especially regarding the effect of modulation of NR4A1 and the JNK/AP-1 pathway on coronavirus replication and pathogenesis, studies will need to be performed on primary cell cultures of more donors. To this end, future experiments should

also include a larger range of viral doses to study the impact of initial infection severity on our findings. Finally, we largely focused on gene expression and our findings would likely benefit from larger scale proteomics approaches to gain further insights in the exact modulation of the signaling pathways by SARS-CoV-2 for example.

Our results also demonstrated an important difference in epithelial transcriptional responses after infection with pathogenic and low pathogenic coronaviruses. Induction of interferon-related genes was less strong by the pathogenic coronavirus strains when compared to low pathogenic HCoV-229E and HCoV-OC43. While an efficient interferon and interferon-stimulated genes response was reported for HCoV-229E and HCoV-OC43 (286), a lower response has been reported previously for pathogenic coronaviruses (287-289) and is also less strong than pathogenic influenza A H1N1 (290). This effect perhaps points to mechanisms of immune evasion through multiple possible mechanisms (291). When our cultures were supplemented with IFN-λ1 during infection, reduced SARS-CoV-2 levels were observed, supporting a role for suppression of interferon-mediated antiviral defenses in the pathogenicity of coronaviruses such as SARS-CoV-2. Recently, Banday and colleagues (292) showed similar results for SARS-CoV-2 using IFN-β and IFN -λ in a colon epithelial cell line (Caco-2), while Feld and colleagues (293) showed in outpatient COVID-19 patients that treatment with pegylated interferon lambda resulted in a more rapid clearance for SARS-CoV-2 compared to the placebo group. Finally, also in bronchial epithelial cell cultures this effect was confirmed using IFN-β1 and IFN-λ2 (294).

If we take all our results together, an interesting difference can be observed between low pathogenic coronaviruses, highly pathogenic coronaviruses with high mortality such as MERS-CoV and SARS-CoV, and with SARS-CoV-2 that is somewhere in between those two severity levels. Low pathogenic coronaviruses show a quick induction of both interferon-related genes and IEGs. Highly pathogenic MERS-CoV and SARS-CoV, that have an increased mortality compared to SARS-CoV-2 (295), show a lack of interferon gene induction but a strong induction of IEGs, whereas SARS-CoV-2 lacks both induction of interferon-related genes and IEGs. These changes could explain how low pathogenic strains are quickly cleared by a strong antiviral response, which combined with rapid induction of IEGs likely results in local inflammation-related symptoms. On the other hand, MERS-CoV and SARS-CoV impair/delay anti-viral defenses, thereby extending infection time, which combined with a quick induction of IEGs, likely results in strong inflammation and related symptoms correlated to the high level of infection. Uniquely, SARS-CoV-2 also impairs anti-viral responses; however; combined with a lack in IEG induction, inflammation is likely only local until the viral titers become so high that the resulting tissue damage promotes inflammation that leads to typical COVID-19 symptoms. This is clearly speculation but in line with the severity of the viruses and translation of these findings into those in human subjects would

be an exciting next step. Additionally, since SARS-CoV-2 is associated with higher levels of asymptomatic infections (295), it would be interesting to investigate if in these patients the interferon response may be present while the induction of IEGs is still absent (296).
The findings from our study highlight differences in transcriptional responses of airway epithelial cells to SARS-CoV-2 infection compared to other coronaviruses. The lack of induction or even suppression of IEGs expression by SARS-CoV-2 was striking and uncharacteristic of previously known coronaviruses and may contribute to its pathogenicity in multiple ways. In addition, lack of transcriptional activation of the interferon pathway is a unique feature that may distinguish highly pathogenic from low pathogenic coronavirus infections. This knowledge can aid in the understanding of SARS-CoV-2 pathogenesis and support development of therapeutic (host-directed) strategies against coronaviruses in general.

Methods

Cell culture

Primary human bronchial epithelial cells (PBEC) were isolated from tumor-free resected bronchus rings obtained from lung cancer patients undergoing a resection surgery at the Leiden University Medical Center (LUMC, Leiden, the Netherlands). Patients from which this lung tissue was derived were enrolled in the biobank via a no-objection system for coded anonymous further use of such tissue (www.coreon.org). Within this framework, individual written informed consent is not needed. Since 01-09-2022, patients are enrolled in the biobank using written informed consent in accordance with local regulations from the LUMC biobank with approval by the institutional medical ethical committee (B20.042/Ab/ab and B20.042/Kb/kb). Donor baseline characteristics are provided in **Table S1**.
PBEC were biobanked as described (297). In short, after 2h of incubation of the bronchial ring in PBS supplemented with protease XIV, cells were scraped off and seeded in Keratinocyte-Serum Free Medium (KSFM, Life-technologies Europe B.V., the Netherlands) containing 0.2 ng/ml Epidermal Growth Factor (hEGF, Gibco, USA), 25 µg/ml Bovine Pituitary Extract (BPE, Life-technologies Europe B.V.), 1 µM isoproterenol (Sigma-Aldrich, USA) and 100 µg/ml primocin (Invivogen, the Netherlands) in 6-well plates (Corning Costar, USA) coated with 30 µg/ml PureCol (Advanced BioMatrix, USA), 5 µg/ml human fibronectin (Promocell, Germany), and 10 µg/ml bovine serum albumin (Fraction V; Thermo Fisher Scientific, USA). After cell cultures had reached 80-90% confluence, cells were harvested

using soft trypsin (Life-technologies Europe B.V.) and soybean trypsin inhibitor (SBTI, Sigma-Aldrich) and stored in liquid nitrogen until further use. Cryopreserved PBEC were thawed and expanded in a coated T75 flask (Greiner Bio- One, the Netherlands) until 80-90% confluency was reached after which cells were seeded in a 12-well cell culture insert (40,000 cells per insert; Transwell®, Corning Costar), coated as described above. Apical and basal sides of inserts were filled with a B/D medium supplemented with 1 nM EC23 (Tocris, UK). B/D medium is a mix of 50% Bronchial Epithelial Cell Medium-basal (BEpiCM-b; ScienCell, Sanbio) and 50% Dulbecco's modified Eagle's medium (DMEM; Stemcell Technologies, Germany) supplemented with 12.5 mM HEPES, bronchial epithelial cell growth supplements, 100 U/ml penicillin, 100 µg/ml streptomycin (all from ScienCell) and 1 mM glutaMAX (Thermo Fisher Scientific). After confluency was reached, the apical medium was removed and cells were cultured at the air-liquid interface (ALI) in B/D medium with 50 nM EC-23 for up to 5 to 6 weeks; medium was refreshed three times a week, each time the apical side was washed with pre-warmed PBS.

Calu-3 cells (ATCC, HTB-55TM) were cultured in Eagle's minimum essential medium (EMEM, Lonza), supplemented with 9% fetal calf serum (FCS; CapriCorn Scientific, USA), 1% non-essential amino acids (NEAA, Sigma-Aldrich), 2 mM L-glutamine (Sigma-Aldrich), 1 mM sodium pyruvate (Sigma-Aldrich) and 100 U/ml of penicillin/ streptomycin (P/S; Sigma-Aldrich). Infections were performed with the same medium, except that 2% FCS was used.
Vero E6 cells (Collection Medical Microbiology, LUMC) were cultured in DMEM with 4.5 g/l glucose with L-glutamin (DMEM; Lonza, Switzerland), supplemented with 8% FCS and 100 U/ml of P/S (Sigma-Aldrich). Infections in Vero E6 cells were performed in EMEM with 25 mM HEPES supplemented with 2% FCS (PAA), 2mM L-glutamine (Sigma-Aldrich), and 100 U/ml of P/S (Sigma-Aldrich).
HUH-7 cells (Collection Medical Microbiology, LUMC) were cultured in DMEM with 4.5 g/l glucose with L-glutamin (DMEM; Lonza, Switzerland), supplemented with 8% FCS, 1% non-essential amino acids (NEAA, Sigma-Aldrich), 2 mM L-glutamine (Sigma-Aldrich) and 100 U/ml of P/S (Sigma-Aldrich). Infections in HUH-7 cells were performed in EMEM with 25 mM HEPES supplemented with 2% FCS (PAA), 2mM L-glutamine (Sigma-Aldrich), and 100 U/ml of P/S (Sigma-Aldrich).
All cell cultures were maintained at 37°C in an atmosphere of 5% CO_2.

Virus stocks

All experiments with SARS-CoV, SARS-CoV-2 or MERS-CoV were performed at the LUMC biosafety level 3 facilities. The clinical isolate SARS-CoV-2/Leiden-0008 was isolated from a

nasopharyngeal sample collected at the LUMC during the first wave of the coronavirus pandemic in March 2020 (GenBank: MT705206.1). SARS-CoV-2/Leiden-0008 (Passage 2) and SARS-CoV isolate Frankfurt 1 (298) (Passage 4) were grown in Vero E6 cells. The SARS-CoV-2 stock was sequenced to exclude Vero cell adaptation in the spike S1/S2 cleavage site. MERS-CoV (N3/Jordan, GenBank: KJ614529.1) (Passage 3) and HCoV-229E (Passage 2, GenBank: NC_002645.1) were grown on HUH-7 cells. HCoV-OC43 was isolated from a bronchioalveolar lavage sample collected between 2018 and 2020 at the LUMC, and grown on primary bronchial epithelial cell cultures at the air-liquid interface. Next-generation sequencing was done and the isolate was mapped to the HCoV-OC43 strain ATCC VR-759 (GenBank: AY585228.1). Virus titers were determined by plaque assay on Vero E6 cells, and for MERS-CoV and HCoV-229E on HUH7 cells, as described before(299). Virus titer of HCoV-OC43 was determined by RT-qPCR, due to the lack of susceptible cells for plaque assay.

Viral infection of ALI-PBEC

The apical side of inserts was washed with 200 µl PBS for 10 min at 37°C to remove excess mucus and basal medium was refreshed prior to infection. Cells were infected with 30,000 plaque-forming units (PFU) of SARS-CoV-2, MERS-CoV, SARS-CoV and HCoV-229E in 200 µl PBS per insert for 2h at 37 °C on a rocking platform (estimated multiplicity of infection [MOI] of 0.03) (300, 301). For HCoV-OC43, the experiments were performed in an independent experiment, however using cultures from the same donors. Infections with HCoV-OC43 were performed at 33 °C and SARS-CoV-2 was taken along as a control at this temperature. The same multiplicity of infection for HCoV-OC43 was used as for the other coronavirus infections, but the titer was based on RT-qPCR measurement of the virus stock, in lack of a good cell culture model to perform a plaque assay experiment. For noninfected (mock) controls the same procedure was performed with PBS only. After removal of the inoculum, the apical side was washed three times with PBS and cells were incubated at 33 °C or 37 °C until sampling at several time points post infection (p.i.). At each sampling time-point, 200 µl of PBS was added to the apical side of the cells, and after incubation for 10 min at 37°C supernatant was harvested for quantification of infectious viral particles by plaque assay and RNA copies by RT-qPCR. Cells were then lysed using 200 µl of RNA lysis buffer (Promega, the Netherlands) or 250 µl Guanidine thiocyanate (GITC) reagent (3 M GITC (Fluka), 2% sarkosyl (Sigma-Aldrich), 50 mM Tris (Affymetrix), 20 mM EDTA (Sigma-Aldrich)) per insert. For long-term SARS-CoV-2 infection, cells were infected with 10^6 PFU of SARS-CoV-2 (estimated MOI of 1) in the same way as described above but the inserts were incubated for 1-7 days.

RNA isolation and quantitative real-time PCR (RT- qPCR)

Total intracellular RNA was robotically extracted using the Maxwell® 16 simply RNA tissue kit (Promega) and quantified using a NanoDrop™ One UV-Vis Spectrophotometer (Thermo Fisher Scientific) and stored at -80 ^{o}C until further use. Extracellular RNA was extracted by magnetic bead isolation. The full procedure for this isolation methods is described in the supplementary materials section.
For viral RNA measurement, the cellular reference gene *PGK1* served as control for intracellular RNA. Primers and Taqman probes for *PGK1* were obtained from a published source (299). Viral RNA was quantified by RT-qPCR using the TaqMan™ Fast Virus 1-Step Master Mix (Thermo Fisher Scientific), with primer concentrations for SARS-CoV-2 and SARS-CoV as described previously (256), for MERS-CoV and HCoV-229E with final primer concentrations of 450 nM each and probe concentrations of 200 nM, and for HCoV-OC43 with final primer concentrations of 1000 nM each and probe concentration of 166 nM. Further details on the qPCR methods related to virus and human genes are described in the supplementary materials section. Primer sequences are summarized in **Table S2**.

RNA sequencing

The quality of total RNA was determined by bioanalyser and sequenced by GenomeScan (Leiden, the Netherlands) using an Illumina NovaSeq6000 sequencer with 20 million paired-end reads per sample. The sequences were then trimmed using the Trimmomatic tool, version 0.33. Two consecutive computational strategies were applied for transcriptome reconstruction. First, the Spliced Transcripts Alignment to a Reference (STAR) version 2.5.3a was used to align and identify all reads that belong to the human genome (GRCh38). Samples were then mapped against respective virus genomes SARS-CoV-2 (NC_045512.2), MERS-CoV (NC_019843.3), SARS-CoV (AY291315.1), HCoV-229E (NC_002645.1) and HCoV-OC43 (NC_006213.1). Originally cultures derived from 5 donors were sequenced; however; one donor did not show transcriptional responses to any of the viruses and was therefore excluded from the dataset. RNA-Seq analysis and cellular deconvolution is outline in the supplementary materials.

Differential expression analysis

RNA-seq analysis was conducted using the R package EdgeR. Differential expression analysis was conducted comparing virus infection at each time point to time-matched no virus

control/mock using the following model (gene expression~ patient ID + cell treatment). For high pathogenic virus analysis, SARS-CoV, MERS-CoV and SARS-CoV-2 were merged together as one group and compared to HCoV-229E. Gene signatures were made using the Gene Set Variation Analysis (GSVA) package (version 1.44.5). Genes that were significantly increased in SARS-CoV, MERS-CoV and HCoV-229E-infected cultures across all time points FOS; NR4A1; FOSB; AC025259.3; EGR3; CYR61; EGR1; AC008894.3; RASD1; EGR2; ZFP36; CTGF; IL6 were used to make a general coronavirus signature. Additionally a general IFN response signature (IFIT1; ISG15; IFI6; OAS1; OASL; IFI44; HERC5; MX2; HERC6; OAS3; DDX58; IRF7; SAMD9; HELZ2; USP18; DDX60; LAMP3; EPSTI1; PLSCR1; EIF2AK2; PARP12; PARP9; PARP14; BST2; TRIM22; IFITM3; IRF9) was used to investigate the overall IFN response of each coronavirus. We compared transcriptional responses of epithelial cultures infected with highly pathogenic coronavirus strains (i.e., SARS-CoV; SARS-CoV-2 and MERS-CoV) with those infected with low pathogenic HCoV-229E and HCoV-OC43 at 24, 48 and 72 hours. Infection with HCoV-OC43 was conducted at 33^{o}C, hence for signature analysis, SARS-CoV-2 infection at 33^{o}C was used as a comparison. For all analyses, expression of a gene was considered significantly different with a Benjamini Hochberg corrected P value <0.05 and a Fold change>|1.5|. For the heatmaps, data was normalized using the function vst DeSeq2 package R.

Statistics

Statistical analysis was performed in GraphPad PRISM 9.0.1 (GraphPad Software Inc., CA). Performed statistical tests are indicated in the Figure legends. Data are shown as mean ± SEM of cultures derived from several donors and differences were considered significant at $p<0.05$.

Acknowledgements

This work was supported by a COVID-19 MKMD grant from the Netherlands Organization for Health Research and Development (ZonMw) and the Dutch Society for the Replacement of Animal Testing (Stichting Proefdiervrij) (grant #114025007), a RSEOH-CAG COVID-19 Rapid Response Research Initiative and a RSEOH-CAG 2021 Extension Grant. C.S-B. is supported by the Coordination for the Improvement of Higher Education Personnel (CAPES) (process no. 88881.171440/2018-01), Ministry of Education, Brazil. Part of this research was supported by the Leiden University Fund (LUF), the Bontius Foundation, and donations from the crowdfunding initiative “wake up to corona”.

Data availability statement

The datasets generated and/or analyzed during the current study will be made available upon publication via the European Genome-phenome Archive (EGA) but are currently available from the corresponding author on reasonable request.

Conflict of interest

All authors declare no competing interest in relation to this manuscript

Authors' contributions

YW, MT, MH, PSH, AD and AF were involved in study design and conceptualization. YW, MT, CS-B, AL DN PH and FB performed experiments. NL FB and AF performed RNA-seq analysis and cellular deconvolution. YW, MT, and AD wrote the manuscript. MH, PSH and AF revised the manuscript.

Corresponding author information:
Dr. Alen Faiz, Respiratory Bioinformatics and Molecular Biology (RBMB), School of Life Sciences, Building 4, Room 04.07.418, Thomas St, Ultimo NSW 2007
University of Technology Sydney, Sydney, Australia
E-mail: alen.faiz@uts.edu.au;
Phone: +61 (0) 420239776

Supplementary Material

Table S1: Donor characteristics

	Donor characteristics	Donor characteristics
	RNA-Seq	**Long-term**
Number of donors	4	3
Male/Female	2/2	2/1
Age (years) mean [SEM]	63.0 [1.1]	66.33 [7.1]
BMI mean [SEM]	31.2 [5.0]	31.1 [2.8]
Smoking status (non-/ex-/smokers)	0/3/1	02-01-2000
FEV1 % pred [SEM]	109.5 [6.1]	75.27 [4.0]

Abbreviations: SEM (standard error of mean); BMI (body mass index); FEV1 (forced expired volume in 1 sec) ; pred (predicted).

Table S2: Primer sequences

Gene	Encoding protein	Sequence forward primer	Sequence reverse primer	Probe
SARS-CoV-2 E	Envelope protein	ACAGGTACGTTAATAGTTAATAGCGT	ATATTGCAGCAGTACGCACACA	TexRed-ACACTAGCCATCCTTACTGCGCTTCG-BHQ1
SARS-CoV-2 RdRp	RNA-dependent RNA polymerase	GTGARATGGTCATGTGTGGCGG	CARATGTTAAASACACTATTAGCATA	FAM-CAGGTGGAACCTCATCAGGAGATGC-BHQ1
MERS-CoV N	Nucleocapsid protein	GTACCTCTTAATGCCAATTC	GAGCCAGTTGCxTTAATTC	TexRed-TCTGTCCTGTCTCCGCCAATAC-BHQ2

HCoV-229E M	Membrane protein	CATACTATCAACCCATTCAACAAG	CACGGCAACTGTCATGTATT	FAM-ATGAACCTGAACACCTGAAGCCAATCTATG-BHQ1
FOSB	FOSB	GCTGCAAGATCCCCTACGAAG	ACGAAGAAGTGTACGAAGGGTT	-
NR4A1	Nuclear receptor 4A1	ATGCCCTGTATCCAAGCCC	GTGTAGCCGTCCATGAAGGT	-
FOS	C-Fos	GGGGCAAGGTGGAACAGTTAT	CCGCTTGGAGTGTATCAGTCA	-
ATP5B	ATP synthase subunit beta	TCACCCAGGCTGGTTCAGA	AGTGGCCAGGGTAGGCTGAT	-
OAZ1	Ornithine decarboxylase antizyme 1	GGATCCTCAATAGCCACTGC	TACAGCAGTGGAGGGAGACC	-

Supplementary tables S3 – S5

The data of Table S3, table S4 and table S5 are shown in an online repository (figshare). Please find the (private) link to access the table below:

https://figshare.com/s/7eea9ca4e79760c369a5

Supplementary Figures

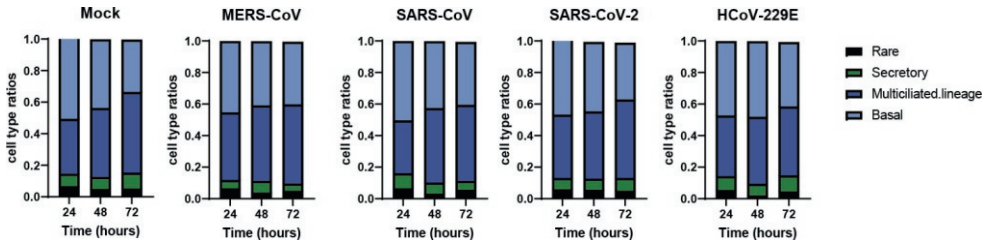

Figure S1: Cellular deconvolution during coronavirus infection of well-differentiated air-liquid interface (ALI) cultures of primary bronchial epithelial cells (PBEC). PBEC that were differentiated for 6 weeks at ALI were infected in parallel with four different coronaviruses. Relative proportion of different cell types of infected cultures over 72h determined by cellular deconvolution of the transcriptomic datasets. N=4 independent donors.

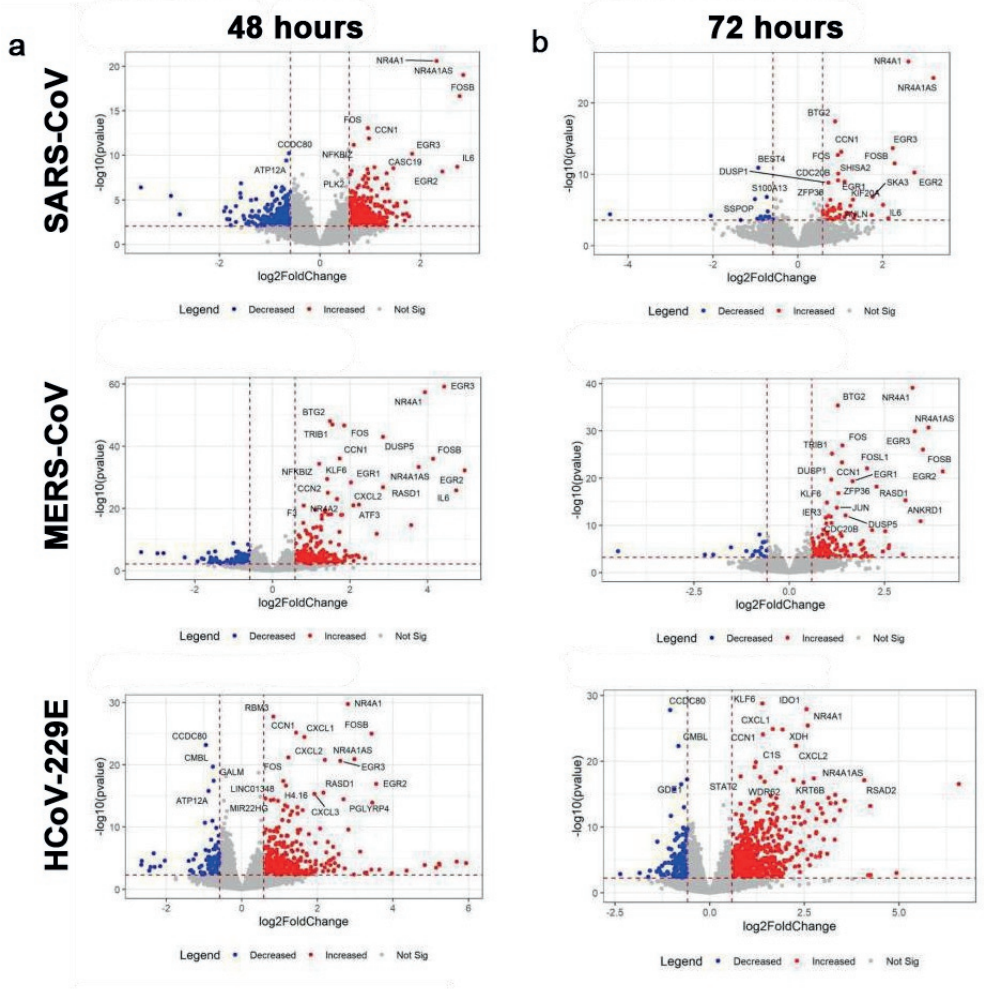

Figure S2: Gene expression profiles of well-differentiated primary bronchial epithelial cell cultures infected with three different coronaviruses. (a) Volcano plots depicting gene expression profiles of bronchial epithelial cell cultures infected with SARS-CoV, MERS-CoV or HCoV-299E after 48 h or (b) 72 h post infection in comparison to the uninfected controls. Red dots indicate significantly upregulated genes and blue dots indicate signficantly downregulated genes. N=4.

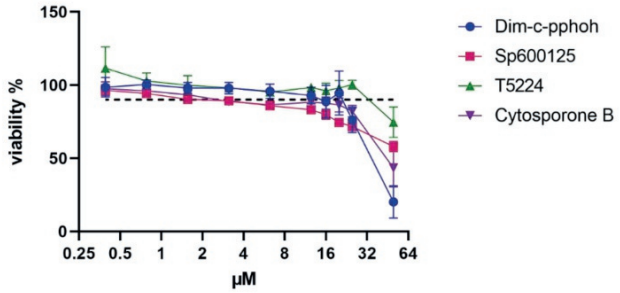

Figure S3: Cytotoxicity of tested JNK/AP-1 signaling modulating compounds on Calu-3 cells. Cell viability was measured by MTS assay after 24 h of treatment. The black dotted line indicates 90% viability. Mean values ± SD are shown, n=4.

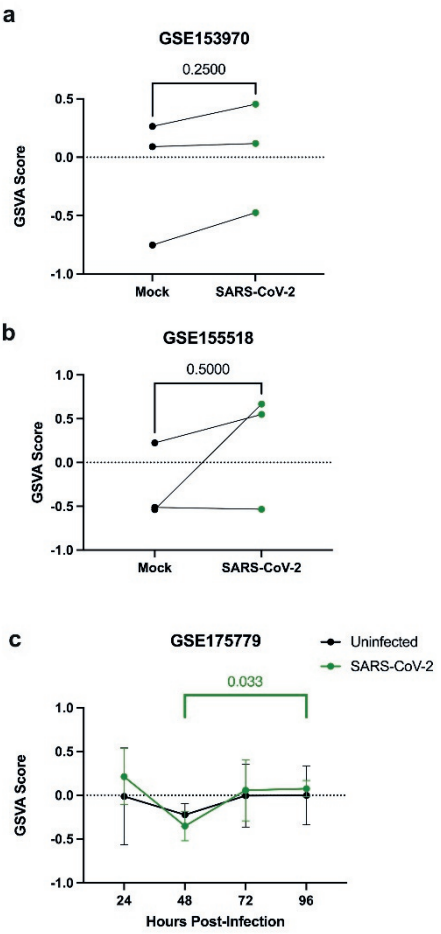

Figure S4: GSVA of IEG gene set on (a) A publicly available dataset (GSE153970) with RNA-seq analysis on primary epithelial cell cultures mock-infected or infected with SARS-CoV-2 at a MOI=0.25 at 48 hpi. (b) A publicly available dataset (GSE155518) derived from primary human lung alveolar epithelial organoid cultures infected with SARS-CoV-2 and assessed at 48 hpi. (c) A publicly available dataset (GSE175779) from primary human bronchial epithelial cells infected with SARS- CoV-2 over a 96 h infection period. Wilcoxon paired nonparametric statistical analysis was conducted on GSE153970 and GSE155518, while two-way ANOVA with Bonferroni correction was performed on GSE175779.

References

1. Zhu Z, Lian X, Su X, Wu W, Marraro GA, Zeng Y. 2020. From SARS and MERS to COVID-19: a brief summary and comparison of severe acute respiratory infections caused by three highly pathogenic human coronaviruses. Respiratory Research 21:224.
2. Abdelghany TM, Ganash M, Bakri MM, Qanash H, Al-Rajhi AMH, Elhussieny NI. 2021. SARS-CoV-2, the other face to SARS-CoV and MERS-CoV: Future predictions. Biomedical Journal 44:86-93.
3. Hamre D, Procknow JJ. 1966. A new virus isolated from the human respiratory tract. Proc Soc Exp Biol Med 121:190-3.
4. McIntosh K, Becker WB, Chanock RM. 1967. Growth in suckling-mouse brain of "IBV-like" viruses from patients with upper respiratory tract disease. Proc Natl Acad Sci U S A 58:2268-73.
5. Lukassen S, Chua RL, Trefzer T, Kahn NC, Schneider MA, Muley T, Winter H, Meister M, Veith C, Boots AW, Hennig BP, Kreuter M, Conrad C, Eils R. 2020. SARS-CoV-2 receptor ACE2 and TMPRSS2 are primarily expressed in bronchial transient secretory cells. The EMBO journal 39:e105114-e105114.
6. Ravindra NG, Alfajaro MM, Gasque V, Habet V, Wei J, Filler RB, Huston NC, Wan H, Szigeti-Buck K, Wang B, Wang G, Montgomery RR, Eisenbarth SC, Williams A, Pyle AM, Iwasaki A, Horvath TL, Foxman EF, Pierce RW, van Dijk D, Wilen CB. 2020. Single-cell longitudinal analysis of SARS-CoV-2 infection in human airway epithelium. PLOS Biol.
7. Aliee H, Massip F, Qi C, Stella de Biase M, van Nijnatten J, Kersten ET, Kermani NZ, Khuder B, Vonk JM, Vermeulen RC. 2022. Determinants of expression of SARS-CoV-2 entry-related genes in upper and lower airways. Allergy 77:690-694.
8. Johansen MD, Mahbub RM, Idrees S, Nguyen DH, Miemczyk S, Pathinayake P, Nichol K, Hansbro NG, Gearing LJ, Hertzog PJ, Gallego-Ortega D, Britton WJ, Saunders BM, Wark PA, Faiz A, Hansbro PM. 2022. Increased SARS-CoV-2 Infection, Protease, and Inflammatory Responses in Chronic Obstructive Pulmonary Disease Primary Bronchial Epithelial Cells Defined with Single-Cell RNA Sequencing. Am J Respir Crit Care Med 206:712-729.
9. Bost P, Giladi A, Liu Y, Bendjelal Y, Xu G, David E, Blecher-Gonen R, Cohen M, Medaglia C, Li H, Deczkowska A, Zhang S, Schwikowski B, Zhang Z, Amit I. 2020. Host-Viral Infection Maps Reveal Signatures of Severe COVID-19 Patients. Cell 181:1475-1488.e12.
10. Chua RL, Lukassen S, Trump S, Hennig BP, Wendisch D, Pott F, Debnath O, Thürmann L, Kurth F, Völker MT, Kazmierski J, Timmermann B, Twardziok S, Schneider S, Machleidt F, Müller-Redetzky H, Maier M, Krannich A, Schmidt S, Balzer F, Liebig J, Loske J, Suttorp N, Eils J, Ishaque N, Liebert UG, von Kalle C, Hocke A, Witzenrath M, Goffinet C, Drosten C, Laudi S, Lehmann I, Conrad C, Sander L-E, Eils R. 2020. COVID-19 severity correlates with airway epithelium–immune cell interactions identified by single-cell analysis. Nature Biotechnology 38:970-979.
11. Otter CJ, Fausto A, Tan LH, Khosla AS, Cohen NA, Weiss SR. 2023. Infection of primary nasal epithelial cells differentiates among lethal and seasonal human coronaviruses. Proc Natl Acad Sci U S A 120:e2218083120.
12. Jha PK, Vijay A, Halu A, Uchida S, Aikawa M. 2020. Gene Expression Profiling Reveals the Shared and Distinct Transcriptional Signatures in Human Lung Epithelial Cells Infected With SARS-CoV-2, MERS-CoV, or SARS-CoV: Potential Implications in Cardiovascular Complications of COVID-19. Front Cardiovasc Med 7:623012.
13. Jang Y, Seo SH. 2020. Gene expression pattern differences in primary human pulmonary epithelial cells infected with MERS-CoV or SARS-CoV-2. Arch Virol 165:2205-2211.
14. Thaler M, Wang Y, van der Does AM, Faiz A, Ninaber DK, Ogando NS, Beckert H, Taube C, Salgado-Benvindo C, Snijder EJ, Bredenbeek PJ, Hiemstra PS, van Hemert MJ. 2023. Impact

of changes in human airway epithelial cellular composition and differentiation on SARS-CoV-2 infection biology. J Innate Immun 15:562-80.
15. Cantuti-Castelvetri L, Ojha R, Pedro LD, Djannatian M, Franz J, Kuivanen S, van der Meer F, Kallio K, Kaya T, Anastasina M. 2020. Neuropilin-1 facilitates SARS-CoV-2 cell entry and infectivity. Science 370:856-860.
16. Bahrami S, Drablos F. 2016. Gene regulation in the immediate-early response process. Adv Biol Regul 62:37-49.
17. Melms JC, Biermann J, Huang H, Wang Y, Nair A, Tagore S, Katsyv I, Rendeiro AF, Amin AD, Schapiro D, Frangieh CJ, Luoma AM, Filliol A, Fang Y, Ravichandran H, Clausi MG, Alba GA, Rogava M, Chen SW, Ho P, Montoro DT, Kornberg AE, Han AS, Bakhoum MF, Anandasabapathy N, Suarez-Farinas M, Bakhoum SF, Bram Y, Borczuk A, Guo XV, Lefkowitch JH, Marboe C, Lagana SM, Del Portillo A, Tsai EJ, Zorn E, Markowitz GS, Schwabe RF, Schwartz RE, Elemento O, Saqi A, Hibshoosh H, Que J, Izar B. 2021. A molecular single-cell lung atlas of lethal COVID-19. Nature 595:114-119.
18. Totura AL, Baric RS. 2012. SARS coronavirus pathogenesis: host innate immune responses and viral antagonism of interferon. Curr Opin Virol 2:264-75.
19. Sa Ribero M, Jouvenet N, Dreux M, Nisole S. 2020. Interplay between SARS-CoV-2 and the type I interferon response. PLoS Pathog 16:e1008737.
20. Rex DAB, Dagamajalu S, Kandasamy RK, Raju R, Prasad TSK. 2021. SARS-CoV-2 signaling pathway map: A functional landscape of molecular mechanisms in COVID-19. J Cell Commun Signal 15:601-608.
21. Guo H, Golczer G, Wittner BS, Langenbucher A, Zachariah M, Dubash TD, Hong X, Comaills V, Burr R, Ebright RY, Horwitz E, Vuille JA, Hajizadeh S, Wiley DF, Reeves BA, Zhang JM, Niederhoffer KL, Lu C, Wesley B, Ho U, Nieman LT, Toner M, Vasudevan S, Zou L, Mostoslavsky R, Maheswaran S, Lawrence MS, Haber DA. 2021. NR4A1 regulates expression of immediate early genes, suppressing replication stress in cancer. Mol Cell 81:4041-4058.e15.
22. Weston CR, Davis RJ. 2007. The JNK signal transduction pathway. Curr Opin Cell Biol 19:142-9.
23. Huang G, Shi LZ, Chi H. 2009. Regulation of JNK and p38 MAPK in the immune system: signal integration, propagation and termination. Cytokine 48:161-9.
24. Ludwig S, Ehrhardt C, Neumeier ER, Kracht M, Rapp UR, Pleschka S. 2001. Influenza virus-induced AP-1-dependent gene expression requires activation of the JNK signaling pathway. J Biol Chem 276:10990-8.
25. Li XM, Sun SZ, Wu FL, Shi T, Fan HJ, Li DZ. 2016. Study on JNK/AP-1 signaling pathway of airway mucus hypersecretion of severe pneumonia under RSV infection. Eur Rev Med Pharmacol Sci 20:853-7.
26. Nacken W, Ehrhardt C, Ludwig S. 2012. Small molecule inhibitors of the c-Jun N-terminal kinase (JNK) possess antiviral activity against highly pathogenic avian and human pandemic influenza A viruses. Biol Chem 393:525-34.
27. Egarnes B, Blanchet MR, Gosselin J. 2017. Treatment with the NR4A1 agonist cytosporone B controls influenza virus infection and improves pulmonary function in infected mice. PLoS One 12:e0186639.
28. Duncan JKS, Xu D, Licursi M, Joyce MA, Saffran HA, Liu K, Gohda J, Tyrrell DL, Kawaguchi Y, Hirasawa K. 2023. Interferon regulatory factor 3 mediates effective antiviral responses to human coronavirus 229E and OC43 infection. Front Immunol 14:930086.
29. Lei X, Dong X, Ma R, Wang W, Xiao X, Tian Z, Wang C, Wang Y, Li L, Ren L, Guo F, Zhao Z, Zhou Z, Xiang Z, Wang J. 2020. Activation and evasion of type I interferon responses by SARS-CoV-2. Nat Commun 11:3810.

30. Siu KL, Yeung ML, Kok KH, Yuen KS, Kew C, Lui PY, Chan CP, Tse H, Woo PC, Yuen KY, Jin DY. 2014. Middle east respiratory syndrome coronavirus 4a protein is a double-stranded RNA-binding protein that suppresses PACT-induced activation of RIG-I and MDA5 in the innate antiviral response. J Virol 88:4866-76.
31. Frieman M, Ratia K, Johnston RE, Mesecar AD, Baric RS. 2009. Severe acute respiratory syndrome coronavirus papain-like protease ubiquitin-like domain and catalytic domain regulate antagonism of IRF3 and NF-kappaB signaling. J Virol 83:6689-705.
32. Stolting H, Baillon L, Frise R, Bonner K, Hewitt RJ, Molyneaux PL, Gore ML, Breathing Together C, Barclay WS, Saglani S, Lloyd CM. 2022. Distinct airway epithelial immune responses after infection with SARS-CoV-2 compared to H1N1. Mucosal Immunol 15:952-963.
33. Kim YM, Shin EC. 2021. Type I and III interferon responses in SARS-CoV-2 infection. Exp Mol Med 53:750-760.
34. Banday AR, Stanifer ML, Florez-Vargas O, Onabajo OO, Papenberg BW, Zahoor MA, Mirabello L, Ring TJ, Lee CH, Albert PS, Andreakos E, Arons E, Barsh G, Biesecker LG, Boyle DL, Brahier MS, Burnett-Hartman A, Carrington M, Chang E, Choe PG, Chisholm RL, Colli LM, Dalgard CL, Dude CM, Edberg J, Erdmann N, Feigelson HS, Fonseca BA, Firestein GS, Gehring AJ, Guo C, Ho M, Holland S, Hutchinson AA, Im H, Irby L, Ison MG, Joseph NT, Kim HB, Kreitman RJ, Korf BR, Lipkin SM, Mahgoub SM, Mohammed I, Paschoalini GL, Pacheco JA, Peluso MJ, Rader DJ, Redden DT, Ritchie MD, et al. 2022. Genetic regulation of OAS1 nonsense-mediated decay underlies association with COVID-19 hospitalization in patients of European and African ancestries. Nat Genet 54:1103-1116.
35. Feld JJ, Kandel C, Biondi MJ, Kozak RA, Zahoor MA, Lemieux C, Borgia SM, Boggild AK, Powis J, McCready J, Tan DHS, Chan T, Coburn B, Kumar D, Humar A, Chan A, O'Neil B, Noureldin S, Booth J, Hong R, Smookler D, Aleyadeh W, Patel A, Barber B, Casey J, Hiebert R, Mistry H, Choong I, Hislop C, Santer DM, Lorne Tyrrell D, Glenn JS, Gehring AJ, Janssen HLA, Hansen BE. 2021. Peginterferon lambda for the treatment of outpatients with COVID-19: a phase 2, placebo-controlled randomised trial. Lancet Respir Med 9:498-510.
36. Vanderwall ER, Barrow KA, Rich LM, Read DF, Trapnell C, Okoloko O, Ziegler SF, Hallstrand TS, White MP, Debley JS. 2022. Airway epithelial interferon response to SARS-CoV-2 is inferior to rhinovirus and heterologous rhinovirus infection suppresses SARS-CoV-2 replication. Sci Rep 12:6972.
37. Zhang C, Wang H, Wen Z, Gu M, Liu L, Li X. 2022. Asymptomatic Transmissibility Calls for Implementing a Zero-COVID Strategy to End the Current Global Crisis. Front Cell Infect Microbiol 12:836409.
38. Masood KI, Yameen M, Ashraf J, Shahid S, Mahmood SF, Nasir A, Nasir N, Jamil B, Ghanchi NK, Khanum I, Razzak SA, Kanji A, Hussain R, M ER, Hasan Z. 2021. Upregulated type I interferon responses in asymptomatic COVID-19 infection are associated with improved clinical outcome. Sci Rep 11:22958.
39. Amatngalim GD, Schrumpf JA, Dishchekenian F, Mertens TCJ, Ninaber DK, van der Linden AC, Pilette C, Taube C, Hiemstra PS, van der Does AM. 2018. Aberrant epithelial differentiation by cigarette smoke dysregulates respiratory host defence. Eur Respir J. 51:1701009.
40. Drosten C, Günther S, Preiser W, Van Der Werf S, Brodt H-R, Becker S, Rabenau H, Panning M, Kolesnikova L, Fouchier RA. 2003. Identification of a novel coronavirus in patients with severe acute respiratory syndrome. New England journal of medicine 348:1967-1976.
41. Kovacikova K, Morren BM, Tas A, Albulescu IC, van Rijswijk R, Jarhad DB, Shin YS, Jang MH, Kim G, Lee HW. 2020. 6′-β-Fluoro-homoaristeromycin and 6′-fluoro-homoneplanocin A are potent inhibitors of chikungunya virus replication through their direct effect on viral nonstructural protein 1. Antimicrobial Agents and Chemotherapy 64:e02532-19.

42. Mantlo E, Bukreyeva N, Maruyama J, Paessler S, Huang C. 2020. Antiviral activities of type I interferons to SARS-CoV-2 infection. Antiviral Res 179:104811.
43. Mache C, Schulze J, Holland G, Bourquain D, Gensch JM, Oh DY, Nitsche A, Durrwald R, Laue M, Wolff T. 2022. SARS-CoV-2 Omicron variant is attenuated for replication in a polarized human lung epithelial cell model. Commun Biol 5:1138.
44. Corman VM, Landt O, Kaiser M, Molenkamp R, Meijer A, Chu DK, Bleicker T, Brunink S, Schneider J, Schmidt ML, Mulders DG, Haagmans BL, van der Veer B, van den Brink S, Wijsman L, Goderski G, Romette JL, Ellis J, Zambon M, Peiris M, Goossens H, Reusken C, Koopmans MP, Drosten C. 2020. Detection of 2019 novel coronavirus (2019-nCoV) by real-time RT-PCR. Euro Surveill 25.